

Inhibitory effects of safranal on laser-induced choroidal neovascularization and human choroidal microvascular endothelial cells and related pathways analyzed with transcriptome sequencing

Qin-Xiao¹, Yao-Yao Sun², Zhan-Jun Lu¹, Tian-Zi Zhang¹, Shan-Shan Li¹, Ting Hua³, Suriguga³, Wen-Lin Chen³, Lin-Lin Ran³, Wen-Zhen Yu², Fei Yang⁴, Burenbatu⁵

¹Department of Ophthalmology, Affiliated Hospital of Inner Mongolia University for Nationalities, Tongliao 028007, Inner Mongolia Autonomous Region, China

²Department of Ophthalmology, Peking University People's Hospital, Beijing 100044, China

³College of Mongolian Medicine, Inner Mongolia University for Nationalities, Tongliao 028000, Inner Mongolia Autonomous Region, China

⁴Department of Ophthalmology, Peking University International Hospital, Beijing 100026, China

⁵Department of Hematology, Affiliated Hospital of Inner Mongolia University for Nationalities, Tongliao 028007, Inner Mongolia Autonomous Region, China

Co-first authors: Qin-Xiao and Yao-Yao Sun

Correspondence to: Burenbatu. Department of Hematology, Affiliated Hospital of Inner Mongolia University for Nationalities, No.1742 East Huolinhe Avenue, Tongliao 028007, Inner Mongolia Autonomous Region, China. dr_burenbatu@126.com

Received: 2021-02-18 Accepted: 2021-04-14

Abstract

• **AIM:** To determine the effects of safranal on choroidal neovascularization (CNV) and oxidative stress damage of human choroidal microvascular endothelial cells (HCVECs) and its possible mechanisms.

• **METHODS:** Forty-five rats were used as a laser-induced CNV model for testing the efficacy and safety of safranal (0.5 mg/kg-d, intraperitoneally) on CNV. CNV leakage on fluorescein angiography (FA) and CNV thickness on histology was compared. HCVECs were used for a H₂O₂-induced oxidative stress model to test the effect of safranal *in vitro*. MTT assay was carried to test the inhibition rate of safranal on cell viability at different concentrations. Tube formation was used to test protective effect of safranal on angiogenesis at different concentrations.

mRNA transcriptome sequencing was performed to find the possible signal pathway. The expressions of different molecules and their phosphorylation level were validated by Western blotting.

• **RESULTS:** On FA, the average CNV leakage area was 0.73±0.49 and 0.31±0.11 mm² ($P=0.012$) in the control and safranal-treated group respectively. The average CNV thickness was 127.4±18.75 and 100.6±17.34 μm ($P=0.001$) in control and safranal-treated group. Under the condition of oxidative stress, cell proliferation was inhibited by safranal and inhibition rates were 7.4%-35.4% at the different concentrations. For tube formation study, the number of new branches was 364 in control group and 35, 42, and 17 in 20, 40, and 80 μg/mL safranal groups respectively ($P<0.01$). From the KEGG pathway bubble graph, the PI3K-AKT signaling pathway showed a high gene ratio. The protein expression was elevated of insulin receptor substrate (IRS) and the phosphorylation level of PI3K, phosphoinositide-dependent protein kinase 1/2 (PDK1/2), AKT and Bcl-2 associated death promoter (BAD) was also elevated under oxidative stress condition but inhibited by safranal.

• **CONCLUSION:** Safranal can inhibit CNV both *in vivo* and *in vitro*, and the IRS-PI3K-PDK1/2-AKT-BAD signaling pathway is involved in the pathogenesis of CNV.

• **KEYWORDS:** choroidal neovascularization; safranal; human choroidal microvascular endothelial cells; oxidative stress; transcriptomics

DOI: 10.18240/ijo.2021.07.04

Citation: Xiao-Qin, Sun YY, Lu ZJ, Zhang TZ, Li SS, Hua T, Suriguga, Chen WL, Ran LL, Yu WZ, Yang F, Burenbatu. Inhibitory effects of safranal on laser-induced choroidal neovascularization and human choroidal microvascular endothelial cells and related pathways analyzed with transcriptome sequencing. *Int J Ophthalmol* 2021;14(7):981-989

INTRODUCTION

Age-related macular degeneration (AMD), which usually occurs successively in both eyes, is mainly manifested by visual deformation, central darkening and decreased contrast. The incidence of AMD is as high as 13% and accounts for approximately 20% of the etiology of blindness among people 65y or older. Estimated 200 million people are affected by AMD all around the world in 2020^[1]. Among AMD types, wet (neovascularization or exudative) AMD accounts for 10%-15% of late-stage AMD patients and is associated with approximately 90% of AMD-related vision loss^[2]. The main pathological mechanism of wet AMD is the formation of choroidal neovascularization (CNV), which leads to the leakage and bleeding of blood vessels and choroidal scars, and further affects vision. Studies have proven that the occurrence of CNV is the result of an imbalance between angiogenic factors and anti-angiogenic factors. Vascular endothelial growth factor (VEGF) is a classic neovascularization factor with high specificity for vascular endothelial cells. It is the main growth factor promoting revascularization and plays an important role in the occurrence of CNV^[3-4].

Oxidative stress also plays an important role in the formation of CNV^[5-6]. Oxidative stress^[5], which is defined as the imbalance of the internal oxidation system and antioxidant system, is correlated to the cause and prognosis of many vascular diseases and is also a primary contributor to AMD. Retinal laser therapy was first introduced to treat AMD^[7]. However, the consequent scar can lead to severe loss of vision. Anti-VEGF factor agents is approved as therapeutic agents treating CNV, however, frequent injection is needed and ocular complications, including endophthalmitis is inevitable. Other treatment modalities, such as anti-inflammation therapy, are still under study on experimental models and are not yet applied to humans^[8]. Thus, development of new therapy targets is needed. Safranal, which systematic name is 2,6,6-trimethylcyclohexa-3,1-din-1-carboxaldehyde, is a volatile carboxaldehyde compound^[9] and is a major constituent of saffron. Safranal has a wide spectrum of biological activities, such as antioxidant, antigenotoxic, anticancer, anti-inflammatory and so on^[10]. Safranal has exhibited antioxidant and anti-apoptotic properties on the central nervous system, especially showing considerable neuroprotective effects. According to previous studies, safranal demonstrated protective effects against oxidative stress and the possible mechanism may be the induction of total antioxidant and capacity sulfhydryl content, with the decrease of malondialdehyde level^[11]. As we mentioned above, good regulation of oxidative stress can promote angiogenesis and tissue repair^[12]. Oxidative stress can promote inflammatory reactions, further promoting the formation of CNV and thus antioxidant stress has become a target of CNV treatment.

Considering that, safranal may exert a protective effect on CNV through its antioxidant stress effect. Although safranal has been studied previously^[13], its inhibitory effect on CNV needs to be confirmed *in vivo* and *in vitro*. So far, only early AMD clinical studies are carried out^[14]. In terms of basic research, however, only light exposure-induced damage models on rats are investigated^[14]. Considering the potential therapeutic effects of safranal on CNV, a laser-induced CNV model is necessary to verify our hypothesis, which to our knowledge hasn't been reported before.

In this study, we aimed to determine whether safranal could inhibit CNV both *in vivo* and *in vitro* and the underlying mechanism of its inhibitory effect. We confirmed the inhibitory effect of safranal on CNV through both a laser-induced CNV animal model *in vivo* and on cellular oxidative stress *in vitro* with human choroidal microvascular endothelial cells (HCVECs). Finally, using transcriptome sequencing, we found and validated the possible pathway involved.

MATERIALS AND METHODS

Ethical Approval This study was performed according to international, national and institutional rules for medical experimental animals use and was approved by the Ethical Committee of Affiliated Hospital of Inner Mongolia University for Nationalities.

Animals Specific, pathogen-free female Brown Norway (BN) rats weighing 150±10 g were purchased from Beijing Weitonglihua Experimental Animal Technology Co., Ltd. Animal care and experiments were conducted under institutional guidelines, and food and tap water were provided *ad libitum*.

Forty-five rats were divided into three groups: 1) blank control group ($n=15$); 2) laser-induced CNV model group ($n=15$); 3) safranal treated CNV model group ($n=15$). A CNV model was developed in all rats of group 2 and 3 with laser treatment (532 nm, 150 mW, 100ms, 100 μ m; Coherent 130SL; Coherent, Santa Clara, CA, USA). Four lesions around the optic disc were made on one eye of each rat, with the other eye used as the control. Intraperitoneal (i.p.) injection was carried out immediately after laser photocoagulation. According to references, the common dose for i.p. injection of safranal was 0.5 mg/kg·d^[15-17]. Thus rats in group 3 were treated by the i.p. injection of safranal (0.5 mg/kg·d) once a day for 21d and phosphate balanced solution (PBS) in group 2 as model control^[18]. After 21d, CNV leakage was assessed by fluorescein angiography (FA) and histology to determine which group was more likely to develop CNV^[19].

Measurement of Choroidal Neovascularization on Fluorescein Angiography FA was performed on day 21 after laser photocoagulation using a digital imaging system (Micro IV, Phoenix, Phoenix City, Arizona, USA) as described previously. Fluorescein (5%, 0.2 mL) was administered i.p.

after the rats were anesthetized and FA was performed after pupil dilation. Both early-phase (1min after injection) and late-phase (10min after injection) fundus angiograms were analyzed. FA were evaluated quantitatively, and the leakage area of each lesion was measured with Image J software^[19].

Histological Analysis and Choroidal Neovascularization Size Measurement Twenty-one days after laser photocoagulation, the eyeballs were removed and were fixed in 4% paraformaldehyde for 24h at room temperature. After removal of the anterior segments, the posterior eyecups were embedded in paraffin. Sagittal sections of 6 μm were cut through the center of the eye at the site of laser photocoagulation. The sections were stained by hematoxylin and eosin (H&E) and assessed by light microscopy (LEICA DFC 300FX, Leica, Solms, Germany). A computer-assisted image analysis system was used to estimate neovascularization based on the thickness of CNV. Measurements were performed on four sections from each laser photocoagulation site^[20].

Cell Culture and Grouping HCVECs (YBio Biotech Co.,Ltd, Shanghai, China) were used in this study. In vitro assays described herein were performed, including the assessment of cell proliferation and tube formation. All other reagents were purchased from Sigma-Aldrich (St. Louis, MO, USA). H_2O_2 was added at 25 $\mu\text{mol/L}$ as an oxidative stress model.

Cell Viability Cellular viability of HCVECs was analyzed using MTT assay (MTT Cell Proliferation and Cytotoxicity Assay Kit; Beyotime, Shanghai, China) according to the manufacturer's instructions and as previously reported^[21-22]. Cells were plated at 5×10^4 per well in 96-well plates, and cell proliferation was measured. H_2O_2 was added at 10 μL (25 $\mu\text{mol/L}$) as an oxidative stress model. 10 μL (10, 20, 40, 80, 160, 320, 640, 800, 1000 $\mu\text{g/mL}$, separately) safranal were added as experimental groups and 10 μL PBS was set as the blank control. Cells were cultured at 37°C overnight. 10 μL MTT was added into each well and incubated at 37°C for 4h and then the absorbance (A) of each well was estimated at 568 nm. Each experiment was repeated in five wells and was duplicated at least three times. OD (optical density) values were obtained, and the inhibition rate was calculated as $(1 - \text{OD}_{\text{experiment group}} / \text{OD}_{\text{negative control group}}) \times 100\%$ ^[23].

Tube Formation Cells at a density of 2×10^5 /well after 10 μL safranal (20, 40, 80 $\mu\text{g/mL}$, separately) treated for 24h with 10 μL PBS as the blank control. According to the manufacturer's instructions and our previous report, 150 μL Matrigel (Cat# 354234; BD Sciences, Franklin Lakes, NJ) solution was poured into 48-well plates and then incubated at 37°C for 0.5h. The HCVECs (5×10^4 per well) were seeded on the Matrigel and cultured for 2-8h. Networks in the Matrigel were counted and photographed. The number of new branches and new branch nodes were measured using Image J software (National

Institutes of Health, Bethesda, MD). The experiments were repeated three times^[21,23-24].

Transcriptome Sequencing The cells were counted and divided into three groups: 1) blank control; 2) H_2O_2 (10 μL , 25 $\mu\text{mol/L}$) treated as an oxidative stress model; 3) oxidative stress model with safranal (10 μL , 40 $\mu\text{g/mL}$) as treated group. Cells were cultured as described above. RNA samples were extracted and identified as previously reported^[21,24]. mRNA was enriched with oligo(dT)-coupled magnetic beads, single-stranded cDNA was synthesized with random hexamers, and double-stranded cDNA was synthesized with buffer, dNTPs, DNA polymerase I and RNase H. The purified double-stranded cDNA was first repaired at the end, followed by A tail addition and connection to the sequencing connector, and then the fragment size was selected using AMPure XP beads. Finally, PCR amplification was performed and the PCR products were purified using AMPure XP beads to obtain the final library. After the library detection was qualified, different libraries were pooled into the flow cell according to the effective concentration and the requirements of the target dismount data volume. Illumina high-throughput sequencing platform was used for sequencing after cBOT clustering.

Western Blotting HCVECs were counted and divided into three groups: 1) blank control (HCVECs); 2) oxidative stress cell group (HCVECs+ H_2O_2); 3) oxidative stress cell group with safranal added. Total protein was extracted from the cells, and the protein concentration was measured using the Bio-Rad assay kit (Bio-Rad, Hercules, CA, USA). Equal amounts of protein (30 μg) were resolved on 12% Tris-HCl polyacrylamide gels and then were transferred to a PVDF blotting membrane (Millipore, Billerica, MA, USA). After blocking, the membranes were incubated with specific antibodies against insulin receptor substrate (IRS), p-phosphatidylinositol 3-kinase (PI3K), t-PI3K, p-phosphoinositide-dependent protein kinase 1/2 (PDK1/2), t-PDK1/2, p-serine/threonine kinase (AKT), t-AKD and Bcl-2 associated death promoter (BAD; 1:2000, Santa Cruz, CA, USA), and GAPDH (1:2000, Abcam, Cambridge, MA, USA). After washing thoroughly, the blots were incubated with peroxidase-conjugated goat anti-rabbit or anti-mouse secondary antibodies (1:1000, ZSGB-Bio, Beijing, China), the protein bands were visualized by chemiluminescence (Pierce, Rockford, IL, USA). The experiment was repeated three times^[25-26].

Statistical Analysis All of the experiments were repeated three times, and the data were presented as the means \pm standard error of mean (SEM). Statistical analysis was performed by the Student's *t* test between groups and one-way ANOVA among three or more groups. $P < 0.05$ was deemed to indicate statistical significance. All the data analyses were performed using SPSS 17.0 (Chicago, IL, USA).

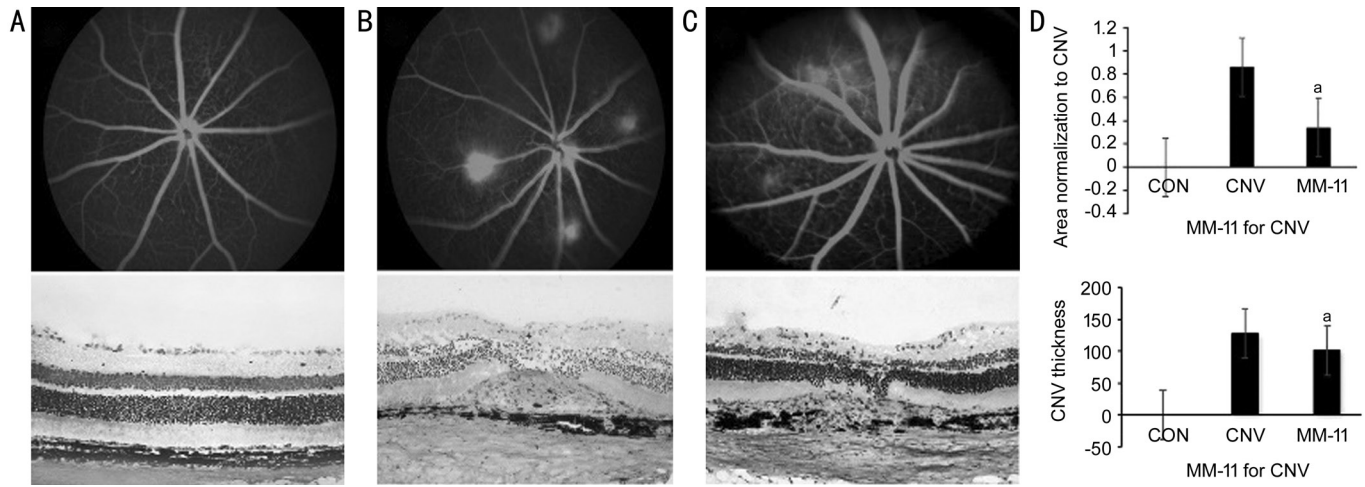


Figure 1 FA and histopathology results showing inhibition of CNV by safranal *in vivo*. Few patches of hyperfluorescence leakage are observed at the lesion site of rats with safranal, but leakage can't be seen in rats in the control groups, with a significant difference. Significant differences are found in the CNV size between the safranal-treated and control groups. The average CNV leakage area is $0.73 \pm 0.49 \text{ mm}^2$ in the PBS group and $0.31 \pm 0.11 \text{ mm}^2$ in the safranal-treated group ($n=15$ in each group, $^aP<0.05$). The inhibition rate is 42.47%. The CNV sections thickness stained with H&E are measured. The average thickness is $127.4 \pm 18.75 \text{ }\mu\text{m}$ in PBS group and $100.6 \pm 17.34 \text{ }\mu\text{m}$ in safranal treated group. A: Blank control; B: PBS control; C: Safranal-treated group; D: Statistical analysis.

RESULTS

Inhibition of Safranal in Choroidal Neovascularization Formation *in vivo*

Two methods were carried out to measure CNV: FA *in vivo*, and CNV thickness on histological analysis. Basically, 4 laser spots were carried out in each eye around the optic nerve. On day 21 after laser-induced CNV, 56 CNVs were successfully induced in 15 eyes in the PBS group, while 54 CNVs in the safranal-treated group. There was no significant difference between the two groups on CNV induction rate ($P<0.05$). CNV leakage area on FA was measured. The average CNV leakage area was $0.73 \pm 0.49 \text{ mm}^2$ in the PBS group and $0.31 \pm 0.11 \text{ mm}^2$ in the safranal-treated group ($P=0.012$). The inhibition rate was 42.47%. These results demonstrated that safranal-treated rat model showed less fluorescein leakage on FA analysis compared with the control rats. Histopathology was also performed comparing the CNV size between the safranal-treated and control groups. The CNV sections thickness stained with H&E were measured. The average thickness was $127.4 \pm 18.75 \text{ }\mu\text{m}$ in PBS group and $100.6 \pm 17.34 \text{ }\mu\text{m}$ in safranal treated group. Significant differences were found in the CNV thickness between the safranal-treated and control groups ($P=0.001$; Figure 1).

Inhibitory Effect of Safranal on Oxidative Stress in HCVECs

Cells treated with H_2O_2 as an oxidative model were cultured with $10 \text{ }\mu\text{L}$ safranal (10, 20, 40, 80, 160, 320, 640, 800, 1000 $\mu\text{g/mL}$) compared with the control. Under the condition of oxidative stress, cell proliferation was inhibited, but safranal had a protective effect on cell proliferation inhibition compared with control, and this protective effect was more obvious with the increase of safranal concentration

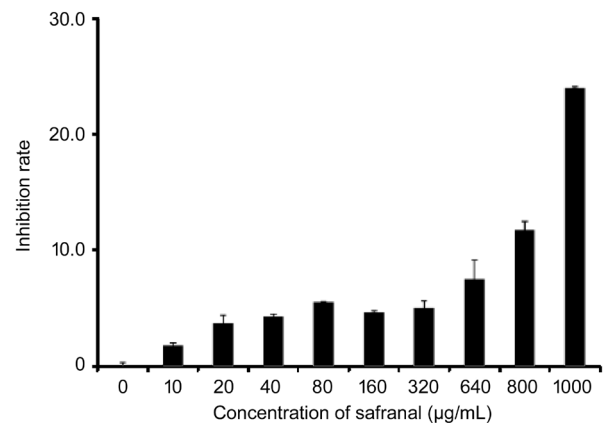


Figure 2 MTT results show an inhibitory effect of safranal on oxidative stress cells *in vitro*.

Cells treated with H_2O_2 as an oxidative model are cultured with $10 \text{ }\mu\text{L}$ safranal (10, 20, 40, 80, 160, 320, 640, 800, 1000 $\mu\text{g/mL}$) compared with the control. The inhibition rates for each group compared with control are 7.4%, 9.7%, 17.7%, 19.0%, 15.3%, 24.1%, 20.9%, 30.5%, and 35.4% separately for different safranal concentrations.

(Figure 2). The inhibition rates for each group compared with control were 7.4%, 9.7%, 17.7%, 19.0%, 15.3%, 24.1%, 20.9%, 30.5% and 35.4% separately for different safranal concentrations.

Inhibition of Tube Formation by Safranal in HCVECs

In the *in vitro* tube formation study, safranal-cultured HCVECs exhibited an impaired capacity to form a regular vascular network. The number of new branches and new branch nodes of the network was also significantly decreased compared with that of the control groups ($P<0.01$). As the concentration of safranal increases, less branch nodes were found (Figure 3). Basically, the number of new branches was 364 in control

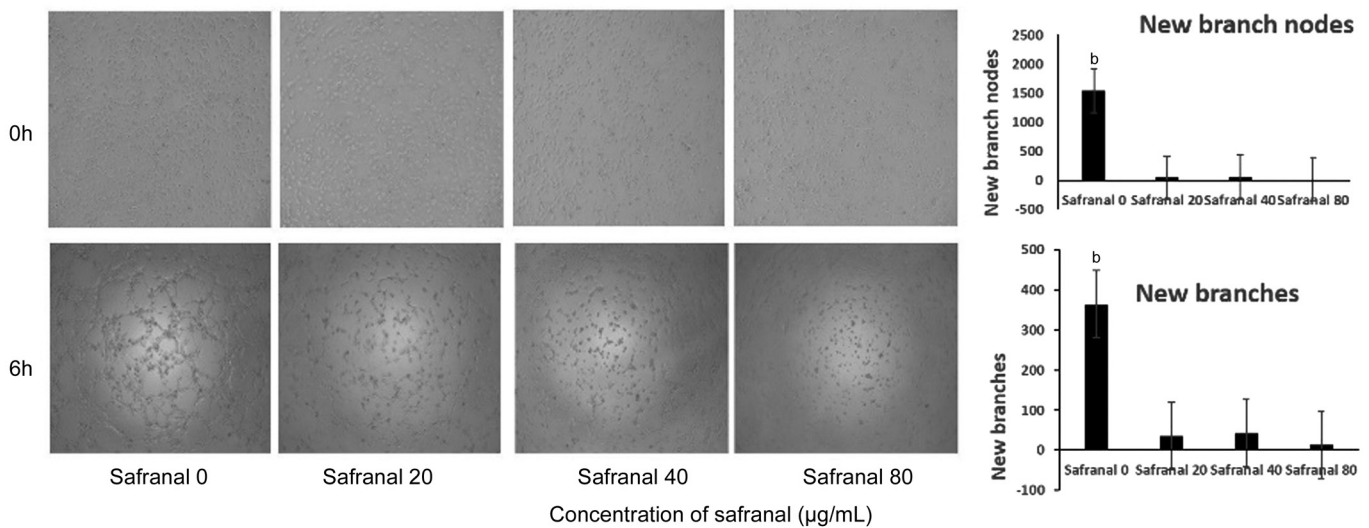


Figure 3 Safranal inhibits tube formation in vitro The number of new branches and new branch nodes of the network is significantly decreased compared with that of the control groups. Basically, the number of new branches is 364 in control group, while the numbers in safranal group are 35 (20 µg/mL), 42 (40 µg/mL), 17 (80 µg/mL), ^b $P < 0.01$. When it comes to the new branches nodes, the new branches nodes is 1543 in the control group and 46 (20 µg/mL), 59 (40 µg/mL), 16 (80 µg/mL) in safranal groups.

group, while the numbers in safranal group were 35, 42, and 17 in 20, 40, and 80 µg/mL respectively ($P < 0.01$). When comes to the new branch nodes, the new branch nodes were 1543 in the control group and 46 (20 µg/mL), 59 (40 µg/mL), 16 (80 µg/mL) in safranal groups (Figure 3).

Inhibition of Oxidative Stress by Safranal Identified with Transcriptome Sequencing Applying the screening criterion established by Cufflinks, the mRNA expression patterns showed differences among the groups as follows [fold change > 2.0 , $P < 0.05$ and false discovery rate (FDR) < 0.05]: compared with the normal control, 85 mRNAs were up-regulated and 93 mRNAs were down-regulated in the oxidative stress group. Compared with the oxidative stress group, 145 mRNAs were up-regulated, and 169 mRNAs were down-regulated in the safranal-treated group.

Comparing the oxidative stress group with the normal control in gene set enrichment analysis, 123 terms were identified about molecular function, 133 terms about cellular component, and 650 terms about biological process. Comparing the safranal-treated group with the oxidative stress group, 123 terms were identified about molecular function, 212 terms about cellular component, and 825 terms about biological process (Figure 4).

When we compared the oxidative stress group with the safranal-treated group, we enriched up to 85 pathways through the Kyoto Encyclopedia of Genes and Genomes (KEGG) pathway and selected the path with a count in the top 15 to obtain the bubble graph. From the KEGG pathway bubble graph, the PI3K-AKT signaling pathway showed a high gene ratio (Figure 5). After analyzing all the data, the IRS-PI3K-PDK1/2-AKT-BAD signaling pathway was found to be

activated in the oxidative stress group and deactivated in the safranal-treated group, suggesting that this signaling pathway may be involved in the treatment of CNV by safranal.

New Gene-gene Interaction Network by Transcriptome Sequencing To obtain more information, differently expressed mRNAs shared between the oxidative stress group and control group and between the safranal-treated group and oxidative stress group were also compared. Key nodes analysis in the gene-gene interaction network was performed, between the closeness centrality of these genes. Four gene-gene interactions were found to be the pivotal nodes in the interaction network, including differences in the expression of CTTN-Pi4k2a, Mtmr7-Larp1p, Mfsd6-Lzic, and ctnd1l-Acadul-Hibch (Figure 6).

IRS-PI3K-PDK1/2-AKT-BAD Signaling Pathway Confirmed by Western Blotting The IRS-PI3K-PDK1/2-AKT-BAD pathway revealed by transcriptome sequencing was verified by Western blot analysis. Basically, Western blot analysis of IRS, t-PI3K, p-PI3K, t-PDK1/2, p-PDK1/2, t-AKT, p-AKT and p-BAD, with GAPDH serves as an internal loading control. We found that under oxidative stress condition, the protein expression was elevated of IRS. Besides, the phosphorylation level of PI3K, PDK1/2, AKT and BAD was also elevated compared with the levels in normal control cells. After safranal treatment, however, the expression level of IRS was down regulated, so did the phosphorylation level of PI3K, PDK1/2, AKT and BAD. As a result, the components of this pathway were subsequently phosphorylated, leading the cells to a BAD-mediated apoptotic signaling pathway (Figure 7).

DISCUSSION

In the present study, we demonstrated that safranal inhibited CNV in a rat model *in vivo*. *In vitro*, the function of safranal

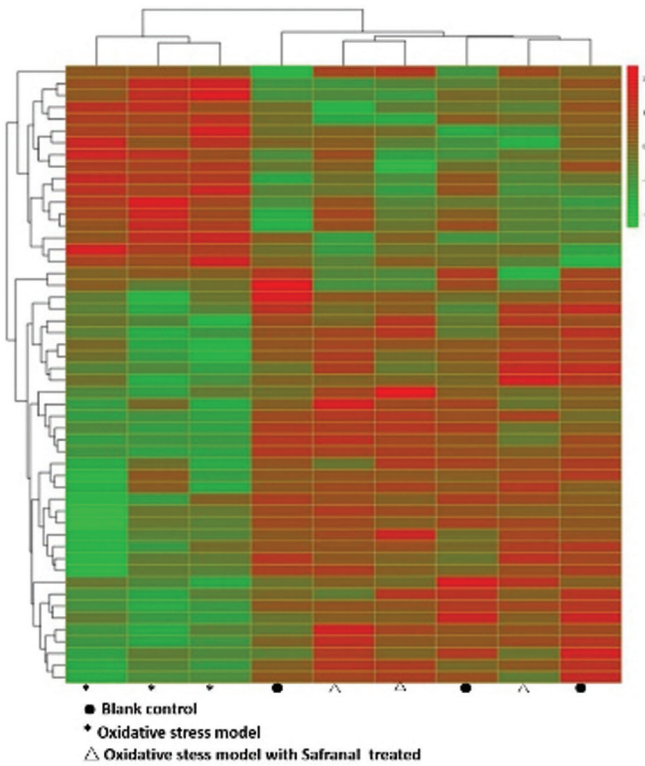


Figure 4 Transcriptome sequencing among the three groups Heatmap colors represent the mean-centered fold-change gene expressions in log-space. The green color represents the down-regulated mRNAs expressions, and the red colors represent up-regulated mRNA expressions. Compared with the normal control, 85 mRNAs were up-regulated, and 93 mRNAs were down-regulated in the oxidative stress group. Compared with the oxidative stress group, 145 mRNAs were up-regulated, and 169 mRNAs were down-regulated in the safranal-treated group.

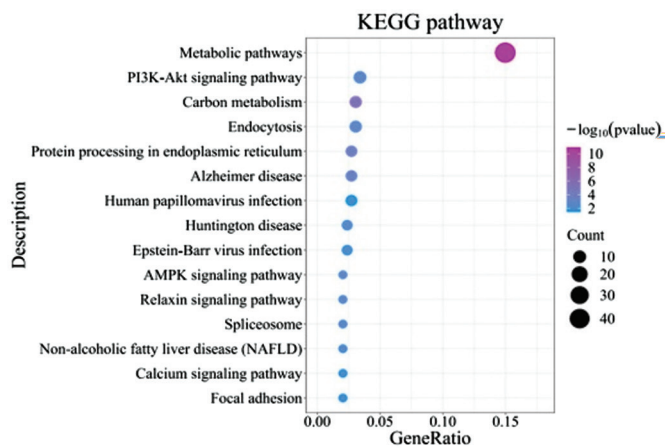


Figure 5 KEGG pathway bubble graph We enrich up to 85 pathways through the KEGG pathway and select the path with a count in the top 15 to obtain the bubble graph. From the KEGG pathway bubble graph, the PI3K-AKT signaling pathway shows a high gene ratio.

was verified in oxidative stress cells and by tube formation studies. Furthermore, the possible signaling pathway was explored by transcriptome sequencing and the IRS-PI3K-PDK1/2-AKT-BAD pathway was identified as being associated

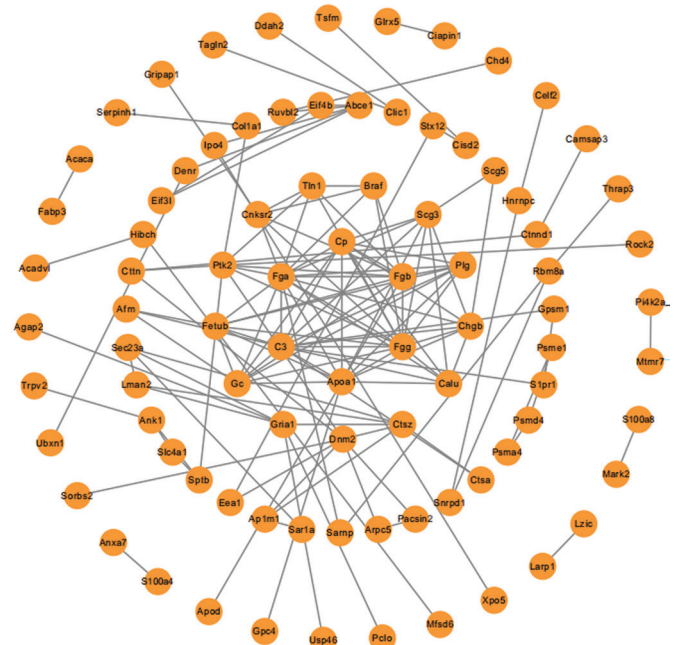


Figure 6 Protein-protein interaction (PPI) network picture The line indicates the interaction between the two genes. The more edges connected to a node, the greater its connectivity, indicating the greater the importance of the node gene in the network. This network diagram shows the common interactions among the three groups in this study to demonstrate the degree of association between genes. The Strings database was used to conduct PPI network interaction analysis on the common DE mRNA, and the cutoff>500 was used as the screening threshold to get the PPI interaction relationship. Four gene-gene interactions were found to be the pivotal nodes in the interaction network, including differences in the expression of CTTN-Pi4k2a, Mtnr7-Larp1p, Mfsd6-Lzic, and ctndnl-Acadul-Hibch.

with oxidative stress in cells and the effect could be inhibited by safranal. These findings suggest that safranal could inhibit CNV mainly through the IRS-PI3K-PDK1/2-AKT-BAD signal pathway. This is the first report concerning the effect of safranal on CNV, and additionally, the signaling pathway was first reported to be associated with CNV.

Currently, the main treatment for CNV is intravitreal injection of anti-VEGF agents. Although many other drugs are still under study, their therapeutic effects still require further investigation. Safranal is a constituent of saffron identified by pharmaceutical studies and has demonstrated antioxidant, anti-inflammatory and antiapoptotic effects^[27]. For example, Alavi *et al*^[28] found the cytoprotective potential of safranal by decreasing ROS accumulation. Malekzadeh *et al*^[18] found that tumor necrosis factor-alpha (TNF- α) levels, Caspase-3 levels and superoxide dismutase (SOD) activity could be inhibited by safranal in diabetic rats. However, no study concerning the effect of safranal on CNV had been studied until the present experiments. Our study found an antioxidant effect on choroidal vessel cells and a destructive effect of angiogenesis *in vivo*

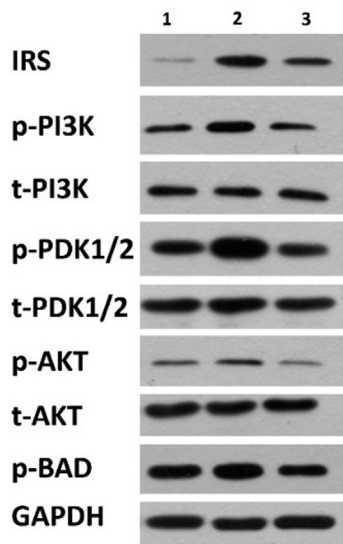


Figure 7 Western blot results showing the phosphorylation change in the IRS-PI3K-PDK1/2-AKT-BAD signaling pathway. The number 1, 2, 3 stand for different groups as follows: 1 for blank control (HCVECs); 2 for oxidative stress cell group; 3 for oxidative stress cell group with safranal added. t-PI3K, t-PDK1/2, and t-AKT stand for the level of total protein levels, while p-PI3K, p-PDK1/2, p-AKT and p-BAD stand for the phosphorylated protein levels. The protein expression was elevated of IRS and the phosphorylation level of PI3K, PDK1/2, AKT and BAD was also elevated under oxidative stress condition but could be inhibited by safranal.

as well. This is the first report on the effect of safranal on neovascularization.

To obtain further knowledge about how safranal function in cells, transcriptome sequencing was carried out. After confirmation by Western blotting, the IRS-PI3K-PDK1/2-AKT-BAD signaling pathway was identified to participate in the oxidative stress process in cells. Additionally, this signaling pathway could be inhibited by safranal. IRS is an important ligand for the insulin response in cells^[29]. Thus far, little research has been conducted on the relationship between IRS and CNV. Cloutier *et al*^[29] found that an antisense oligonucleotide inhibiting IRS-1 expression shows antiangiogenic activity in a CNV model. They also found elevated IRS-1 expression in CNV patients, showing that IRS-1 may be involved in the formation process of both choroidal and retinal neovascularization. These results are consistent with our findings, demonstrating that the IRS signaling pathway is involved in the pathogenesis of CNV and that safranal can effectively reduce IRS expression in the cellular oxidative stress model, thus inhibiting CNV.

Activation of IRS triggers a series of changes in downstream signaling pathways, including the phosphorylation of PI3K. The classical PI3K/AKT signaling pathway^[30-31], is widely involved in cell proliferation, migration, adhesion, apoptosis and angiogenesis. The PI3K/AKT pathway has also been

found to be closely related to the occurrence and development of CNV in ophthalmology. For example, Zhuang *et al*^[32] found that, in retinal CNV models after VEGF treatment, the level of p-AKT was upregulated significantly. A result of PI3K activation is the elevation of BAD, which is also closely related to neovascularization. These are consistent with our findings. Besides, not only IRS but also many other signal transduction pathways are involved in the PI3K/AKT pathway. Whether these other signaling pathways are also involved in safranal's intervention in CNV still needs further study.

Another interesting finding in transcriptome sequencing is that not only the IRS-PI3K-PDK1/2-AKT-BAD signaling pathway was involved in the process of CNV but also some gene expression differences exist based on transcriptome data: including gene expression differences in CTTN-Pi4k2a, Mtmr7-Larp1p, Mfsd6-Lzic, and ctndnl-Acadul-Hibch. Although these genes have not been confirmed to be related to the formation of CNV, some of their characteristics have been found in previous studies. For example, the CTTN gene, which mainly encodes cortactin, is related to angiogenesis and cell proliferation^[33]. MFSD6 and ctndnl are found in the neurons of brain tissue and may be related to energy consumption in the brain^[34]. Whether they are expressed in the retina and the possible functions need further investigation. These gene expression differences may provide directions for further exploration of the pathogenesis of CNV and possible therapeutic targets.

However, this study failed to observe whether inhibition of IRS-PI3K-PDK1/2-AKT-BAD is directly associated with the effect of safranal on CNV. Further studies are needed to clarify the role of this signaling pathway in the protection of CNV by safranal. Also, other possible mechanisms of CNV, such as the VEGF signaling pathway was not investigated in this study. In fact, VEGF has been found to stimulate VEGF-R2/IRS-1/PI3K/AKT axis to regulate endothelial nitric oxide synthase phosphorylation^[35]. The association between VEGF and safranal still needs further investigation. New explorations of the pathogenesis of CNV and possible therapeutic targets require further investigation.

ACKNOWLEDGEMENTS

Foundations: Supported by the National Natural Science Foundation of China (No.81760027; No.81860763); Youth Innovation Project of Affiliated Hospital of Inner Mongolia University for Nationalities (No.2018QNJJ01); Young and Middle-aged Ophthalmic Research Fund of Bethune-Lumitin (No.BJ-LM202005).

Conflicts of Interest: Xiao-Qin, None; Sun YY, None; Lu ZJ, None; Zhang TZ, None; Li SS, None; Hua T, None; Suriguga, None; Chen WL, None; Ran LL, None; Yu WZ, None; Yang F, None; Burenbatu, None.

REFERENCES

- 1 Age-Related Eye Disease Study Research Group. A randomized, placebo-controlled, clinical trial of high-dose supplementation with vitamins C and E, beta carotene, and zinc for age-related macular degeneration and vision loss: AREDS report no. 8. *Arch Ophthalmol* 2001;119(10):1417-1436.
- 2 Sreekumar PG, Hinton DR, Kannan R. The emerging role of senescence in ocular disease. *Oxid Med Cell Longev* 2020;2020:2583601.
- 3 Mettu PS, Allingham MJ, Cousins SW. Incomplete response to anti-VEGF therapy in neovascular AMD: exploring disease mechanisms and therapeutic opportunities. *Prog Retin Eye Res* 2020;100906.
- 4 Pham B, Thomas SM, Lillie E, Lee T, Hamid J, Richter T, Janoudi G, Agarwal A, Sharpe JP, Scott A, Warren R, Brahmabhatt R, MacDonald E, Straus SE, Tricco AC. Anti-vascular endothelial growth factor treatment for retinal conditions: a systematic review and meta-analysis. *BMJ Open* 2019;9(5):e022031.
- 5 Totsuka K, Ueta T, Uchida T, Roggia MF, Nakagawa S, Vavvas DG, Honjo M, Aihara M. Oxidative stress induces ferroptotic cell death in retinal pigment epithelial cells. *Exp Eye Res* 2019;181:316-324.
- 6 Abokyi S, To CH, Lam TT, Tse DY. Central role of oxidative stress in age-related macular degeneration: evidence from a review of the molecular mechanisms and animal models. *Oxid Med Cell Longev* 2020;2020:7901270.
- 7 Virgili G, Bini A. Laser photocoagulation for neovascular age-related macular degeneration. *Cochrane Database Syst Rev* 2007;(3):CD004763.
- 8 Yerramothu P, Vijay AK, Willcox MDP. Inflammasomes, the eye and anti-inflammasome therapy. *Eye (Lond)* 2018;32(3):491-505.
- 9 Rameshrad M, Razavi BM, Hosseinzadeh H. Saffron and its derivatives, crocin, crocetin and safranal: a patent review. *Expert Opin Ther Pat* 2018;28(2):147-165.
- 10 Zeinali M, Zirak MR, Rezaee SA, Karimi G, Hosseinzadeh H. Immunoregulatory and anti-inflammatory properties of *Crocus sativus* (Saffron) and its main active constituents: a review. *Iran J Basic Med Sci* 2019;22(4):334-344.
- 11 Hosseinzadeh H, Sadeghnia HR. Safranal, a constituent of *Crocus sativus* (saffron), attenuated cerebral ischemia induced oxidative damage in rat hippocampus. *J Pharm Pharm Sci* 2005;8(3):394-399.
- 12 Huang YJ, Nan GX. Oxidative stress-induced angiogenesis. *J Clin Neurosci* 2019;63:13-16.
- 13 Cerdá-Bernad D, Valero-Cases E, Pastor JJ, Frutos MJ. Saffron bioactives crocin, crocetin and safranal: effect on oxidative stress and mechanisms of action. *Crit Rev Food Sci Nutr* 2020;1-18.
- 14 Fernández-Albarral JA, de Hoz R, Ramírez AI, López-Cuenca I, Salobrar-García E, Pinazo-Durán MD, Ramírez JM, Salazar JJ. Beneficial effects of saffron (*Crocus sativus* L.) in ocular pathologies, particularly neurodegenerative retinal diseases. *Neural Regen Res* 2020;15(8):1408-1416.
- 15 Erfanparast A, Tamaddonfard E, Taati M, Dabbaghi M. Effects of crocin and safranal, saffron constituents, on the formalin-induced orofacial pain in rats. *Avicenna J Phytomed* 2015;5(5):392-402.
- 16 Bharti S, Golechha M, Kumari S, Siddiqui KM, Arya DS. Akt/GSK-3 β /eNOS phosphorylation arbitrates safranal-induced myocardial protection against ischemia-reperfusion injury in rats. *Eur J Nutr* 2012;51(6):719-727.
- 17 Samarghandian S, Borji A, Delkhosh MB, Samini F. Safranal treatment improves hyperglycemia, hyperlipidemia and oxidative stress in streptozotocin-induced diabetic rats. *J Pharm Pharm Sci* 2013;16(2):352.
- 18 Malekzadeh S, Heidari MR, Razavi BM, Rameshrad M, Hosseinzadeh H. Effect of safranal, a constituent of saffron, on olanzapine (an atypical antipsychotic) induced metabolic disorders in rat. *Iran J Basic Med Sci* 2019;22(12):1476-1482.
- 19 Li SS, Huang L, Sun YY, Bai YJ, Yang F, Yu WZ, Li FT, Zhang Q, Wang B, Geng JG, Li XX. Slit2 promotes angiogenic activity via the Robo1-VEGFR2-ERK1/2 pathway in both *in vivo* and *in vitro* studies. *Invest Ophthalmol Vis Sci* 2015;56(9):5210.
- 20 Sun Y, Yu W, Huang L, Hou J, Gong P, Zheng Y, Zhao M, Zhou P, Li X. Is asthma related to choroidal neovascularization? *PLoS One* 2012;7(5):e35415.
- 21 Zhao M, Bai YJ, Xie WK, Shi X, Li FT, Yang F, Sun YY, Huang L, Li XX. Interleukin-1 β level is increased in vitreous of patients with neovascular age-related macular degeneration (nAMD) and polypoidal choroidal vasculopathy (PCV). *PLoS One* 2015;10(5):e0125150.
- 22 Zhu MH, Liu XJ, Wang SC, Miao J, Wu LC, Yang XW, Wang Y, Kang LH, Li WD, Cui C, Chen H, Sang AM. PKR promotes choroidal neovascularization via upregulating the PI3K/Akt signaling pathway in VEGF expression. *Mol Vis* 2016;22:1361-1374.
- 23 Wu K, Yuan LH, Xia W. Inhibitory effects of apigenin on the growth of gastric carcinoma SGC-7901 cells. *World J Gastroenterol* 2005;11(29):4461-4464.
- 24 Zhu X, Bai Y, Yu W, Pan C, Jin E, Song D, Xu Q, Yao Y, Huang L, Tao Y, Li X, Zhao M. The effects of pleiotrophin in proliferative diabetic retinopathy. *PLoS One* 2015;10(1):e0115523.
- 25 Liu Z, Guo F, Wang Y, Li C, Zhang X, Li H, Diao L, Gu J, Wang W, Li D, He F. BATMAN-TCM: a bioinformatics analysis tool for molecular mechanism of traditional Chinese medicine. *Sci Rep* 2016;6:21146.
- 26 Zhang RZ, Yu SJ, Bai H, Ning K. TCM-Mesh: The database and analytical system for network pharmacology analysis for TCM preparations. *Sci Rep* 2017;7(1):2821.
- 27 Delkhosh-Kasmaie F, Farshid AA, Tamaddonfard E, Imani M. The effects of safranal, a constituent of saffron, and metformin on spatial learning and memory impairments in type-1 diabetic rats: behavioral and hippocampal histopathological and biochemical evaluations. *Biomed Pharmacother* 2018;107:203-211.
- 28 Alavi MS, Fanoudi S, Fard AV, Soukhtanloo M, Hosseini M, Barzegar H, Sadeghnia HR. Safranal attenuates excitotoxin-induced oxidative OLN-93 cells injury. *Drug Res (Stuttg)* 2019;69(6):323-329.

- 29 Cloutier F, Lawrence M, Goody R, Lamoureux S, Al-Mahmood S, Colin S, Ferry A, Conduzorgues JP, Hadri A, Cursiefen C, Udaondo P, Viaud E, Thorin E, Chemtob S. Antiangiogenic activity of aganirsen in nonhuman primate and rodent models of retinal neovascular disease after topical administration. *Invest Ophthalmol Vis Sci* 2012;53(3):1195-1203.
- 30 Xie YB, Shi XF, Sheng K, Han GX, Li WQ, Zhao QQ, Jiang BL, Feng JM, Li JP, Gu YH. PI3K/Akt signaling transduction pathway, erythropoiesis and glycolysis in hypoxia (Review). *Mol Med Rep* 2019;19(2):783-791.
- 31 Jafari M, Ghadami E, Dadkhah T, Akhavan-Niaki H. PI3k/AKT signaling pathway: Erythropoiesis and beyond. *J Cell Physiol* 2019;234(3):2373-2385.
- 32 Zhuang Z, Xiao-qin, Hu H, Tian SY, Lu ZJ, Zhang TZ, Bai YL. Down-regulation of microRNA-155 attenuates retinal neovascularization via the PI3K/Akt pathway. *Mol Vis* 2015;21:1173-1184.
- 33 Ramos-García P, González-Moles MÁ, González-Ruiz L, Ayén Á, Ruiz-Ávila I, Navarro-Triviño FJ, Gil-Montoya JA. An update of knowledge on cortactin as a metastatic driver and potential therapeutic target in oral squamous cell carcinoma. *Oral Dis* 2019;25(4):949-971.
- 34 Bagchi S, Perland E, Hosseini K, Lundgren J, Al-Walai N, Kheder S, Fredriksson R. Probable role for major facilitator superfamily domain containing 6 (MFSD6) in the brain during variable energy consumption. *Int J Neurosci* 2020;130(5):476-489.
- 35 Feliers D, Chen XY, Akis N, Choudhury GG, Madaio M, Kasinath BS. VEGF regulation of endothelial nitric oxide synthase in glomerular endothelial cells. *Kidney Int* 2005;68(4):1648-1659.